Trapezoidal waveguides: first-order propagation equivalence with rectangular waveguides

2007 J. Phys. A: Math. Theor. 40 14555

(http://iopscience.iop.org/1751-8121/40/48/017)

IOP Publishing Journal of Physics A: Mathematical and Theoretical

J. Phys. A: Math. Theor. **40** (2007) 14555–14574 doi:10.1088/1751-8113/40/48/017

Trapezoidal waveguides: first-order propagation equivalence with rectangular waveguides

E M Popescu and S Song

Department of Physics and Computer Science, Wilfrid Laurier University, 75 University Avenue West, Waterloo, Ontario, N2L 3C5, Canada

E-mail: epopescu@wlu.ca and ssong@wlu.ca

Received 2 May 2007, in final form 21 June 2007
Published 14 November 2007
Online at stacks.iop.org/JPhysA/40/14555

Abstract

In the present paper we present in detail a new and improved version of the method of perturbative equivalence between the propagation characteristics of lossless trapezoidal cross-section waveguides and of rectangular cross-section waveguides. The analysis is carried out within the framework of perturbation theory, and to the first order we develop a very simple geometrical argument that allows one to construct for any given waveguide with trapezoidal cross-section an equivalent waveguide with rectangular cross-section. The numerical investigation of our arguments shows excellent agreement between the propagation characteristics of the two equivalent structures.

PACS numbers: 42.60.Da, 42.81.Qb, 42.82.Et

1. Introduction

Trapezoidal cross-sections of semiconductor waveguides—besides specialized applications, e.g. [1]—can be considered with reasonable accuracy to be the most common deviation from the rectangular shape that occurs during the fabrication process of such devices. Indeed, and unless special precautions that are very costly and time consuming are taken (e.g. as in the case of the fabrication of length and height standards in AFM/STM and SEM), the production manufacturing of waveguides will yield, in the general case, structures with profiles that deviate from the rectangular shape. A discussion of the detailed reasons of why such deviations occur is beyond the scope of the present paper, and therefore it will suffice to say that such deviations occur mainly due to the various types of processes involved in the fabrication of the devices (e.g. etching, crystalline plane selective etching, focused ion beam milling, etc).

Under these circumstances, the most frequently encountered deviations from the rectangular geometry are cross-sections with shapes that can be approximated by trapezoidal profiles with reasonable accuracy. Furthermore, and depending on the particular processes involved in the manufacturing of the waveguides, these deviations can range—geometrically

speaking—from negligible to rather substantial [2], and therefore, from the viewpoint of semiconductor optical amplifier (SOA) modeling it is highly desirable for such models to have control—even if at the simplest level—over the geometrical characteristics of the underlying waveguide structure.

In the present paper we will present in detail a simple perturbative treatment of trapezoidal cross-section waveguides that allows one to construct an equivalent rectangular cross-section waveguide that has—to the first order of perturbation—the same propagation characteristics as the original trapezoidal waveguide. The idea of reducing a trapezoidal waveguide to an equivalent rectangular waveguide is by no means new and was originally proposed by Clark and Dunlop [3] in 1988 for rib waveguide structures. In our present work, we apply this idea to the study of strip-loaded waveguide structures, and we derive for this type of structures a very simple and intuitive geometrical method to construct the equivalent rectangular waveguide corresponding to a given trapezoidal waveguide.

One might argue that such a perturbative method for the construction of equivalent waveguides has outlived its usefulness with the advent of modern numerical methods and modern computers. This would indeed be a valid argument if one were to limit oneself only to the study of electromagnetic waveguides. Indeed, more exact theoretical treatments of trapezoidal waveguides exist in the literature [1, 4–6]—although not exceedingly many—which can provide more accurate numerical results than the perturbative method presented here.

However, if one considers the issue of the theoretical description of such waveguides in the broader context of modern design and simulation of optical devices that may contain a large number of SOAs in various operating configurations, one immediately realizes two very important things. On one hand, almost all of the current models of SOAs in the literature (and hence almost all the simulation software for SOA-based optical circuitry) are based on rectangular geometries of the underlying waveguide structures, e.g. [7–9], and on the other hand, current simulation software of SOA-based optical circuitry is complicated and calculationally intensive and extensive enough as it is, such that the addition of another numerical routine that analyzes accurately (i.e. non-perturbatively) the underlying waveguide structure will only result in longer computational times, rendering such simulation software even more time consuming.

With these considerations, the geometrical method for the perturbative construction of equivalent rectangular waveguides that will be described in the present paper allows for a simple generalization of the SOA models extant in the literature to include trapezoidal geometries, and at the same time it allows one to continue to use the already available simulation software (commercial and/or non-commercial) with little or no modification for the design and study of SOA-based circuitry in a more realistic context.

While the purpose of our work is ultimately the generalization of SOA models to include trapezoidal geometries of the underlying waveguide structure, the scope of the present paper is limited to only the description of the perturbative equivalence of rectangular and trapezoidal waveguides. As such, it constitutes the background for theoretical and numerical work which will be reported in a subsequent paper.

The paper is organized as follows. In section 2 we review briefly the perturbative treatment of rectangular waveguides, as a preparatory framework for the perturbative description of the trapezoidal geometry that will be presented in detail in section 3. In section 4 we present the principle underlying the propagation equivalence between trapezoidal and rectangular waveguides, and for the particular case of strip-loaded configurations we derive a simple geometrical method for the construction of the equivalent rectangular waveguide corresponding to a given trapezoidal geometry. In section 5 we present a numerical

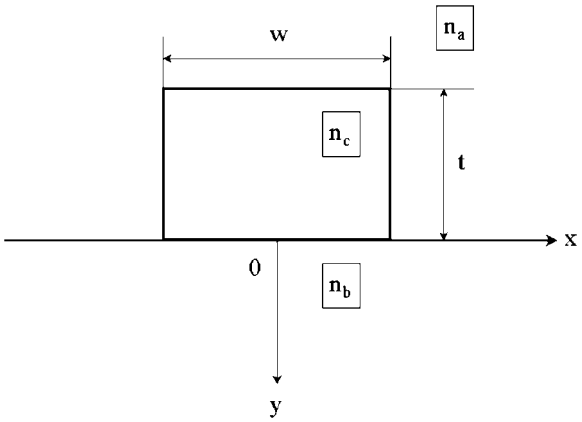

Figure 1. The cross-section of a strip-loaded waveguide structure, with its geometrical and physical characteristics.

investigation of the trapezoidal and corresponding equivalent rectangular geometries, and in section 6 we conclude the paper with a discussion of our results.

2. The perturbative treatment of strip-loaded rectangular waveguides

In this section we briefly review the perturbative modal analysis of rectangular waveguides, with emphasis on the description of strip-loaded waveguide configurations which are the structures of interest for our present work. Since the treatment is largely based on the work done in [10, 11], for comparison and clarity reasons we will attempt in all of the following to preserve as much as possible the same notations and diagrammatics that have been used in these references.

The strip-loaded waveguide configuration is illustrated in figure 1 where the geometrical characteristics of the waveguide are described by its width w and thickness t, and the physical characteristics of the configuration are described by the dimensionless dielectric constants n_a^2, n_b^2 and n_c^2. The quantities n_a, n_b and n_c are respectively the refractive indices of the 'cladding', of the substrate and of the waveguide.

In the perturbative framework, this configuration is obtained from what will be called in all of the following as the 'fundamental' rectangular waveguide configuration, i.e. from a waveguide structure with identical geometrical dimensions, and a distribution of the dielectric constant as illustrated in figure 2.

The use of an auxiliary configuration for the modal analysis of the strip-loaded waveguides is due to the fact that the configuration in figure 2 is analytically solvable, and as such it constitutes the appropriate starting point for the perturbative analysis of the structure in figure 1. Indeed, it is well known from the elementary theory of dielectric waveguides (see for example [12, 13]) that the solution of the Maxwell equations for dielectric waveguide structures in the absence of loss and/or gain sources and for harmonic waves propagating in the z-direction (i.e. in the direction perpendicular to the cross-sectional planes shown in figures 1 and 2) can be functionally reduced to the solution of a single scalar-wave equation of the form

$$\frac{\partial^2 \Psi(x, y)}{\partial^2 x} + \frac{\partial^2 \Psi(x, y)}{\partial^2 y} + \left[k_0^2 n^2(x, y) - \beta_0^2\right] \Psi(x, y) = 0 \tag{2.1}$$

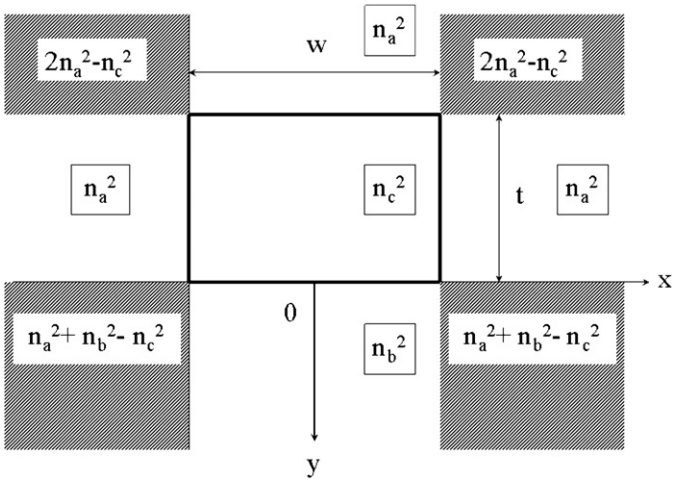

Figure 2. The cross-section of the 'fundamental' rectangular structure which constitutes the basis of the construction of a strip-loaded waveguide in figure 1.

where $\Psi(x, y)$ can be any of the two fields corresponding to the propagation modes E^x_{pq} and E^y_{pq} in the Marcatili notation [13, 14], k_0 is the magnitude of the vacuum propagation vector of the electromagnetic wave and $n^2(x, y)$ is the distribution of the (dimensionless) dielectric function of the waveguide structure.

For the particular fundamental structure in figure 2, the distribution of the dielectric constant can be written in the form

$$n_0^2(x, y) = n_1^2(x) + n_2^2(y) - n_c^2 \tag{2.2}$$

where $n_1^2(x)$ and $n_2^2(y)$ are given by the expressions

$$n_1^2(x) = \begin{cases} n_c^2, & \text{for} \quad |x| < w/2 \\ n_a^2, & \text{for} \quad |x| > w/2 \end{cases} \tag{2.3}$$

$$n_2^2(y) = \begin{cases} n_a^2, & \text{for} \quad y \in (-\infty, -t) \\ n_c^2, & \text{for} \quad y \in (-t, 0) \\ n_b^2, & \text{for} \quad y \in (0, \infty). \end{cases} \tag{2.4}$$

The coordinate separability of the dielectric constant distribution allows for the separability of the scalar-wave equation (2.1), and by setting $\Psi(x, y) = X(x)Y(y)$, the latter reduces to the following system of uncoupled linear differential equations:

$$\begin{cases} \dfrac{d^2X(x)}{dx^2} + \left[k_0^2 n_1^2(x) - \beta_1^2\right] X(x) = 0 \\ \dfrac{d^2Y(y)}{dy^2} + \left[k_0^2 n_2^2(y) - \beta_2^2\right] Y(y) = 0. \end{cases} \tag{2.5}$$

In (2.5), $X(x)$ and $Y(y)$ can be symmetric or antisymmetric functions of x and y respectively, and the separation constants β_1 and β_2 must obey the condition

$$\beta_0^2 = \beta_1^2 + \beta_2^2 - k_0^2 n_c^2. \tag{2.6}$$

Restricting ourselves only to the analysis of the $E_{pq}{}^{x}$ modes of the waveguide, and assuming that the fields are harmonic inside the waveguide, evanescent in the material surrounding the waveguide and symmetric with respect to the x coordinate, one can solve equations (2.5) in a straightforward manner for each of the sectors that correspond to the distribution of the dielectric constant in (2.3) and (2.4). The boundary conditions that are compatible with the modal configuration chosen above are

$$\begin{aligned} &n^2\Psi,\ \frac{\partial\Psi}{\partial x}\text{continuous at } x=\pm w/2\\ &\Psi,\ \frac{\partial\Psi}{\partial y}\text{continuous at } y=0,-t \end{aligned} \tag{2.7}$$

and with these boundary conditions, it can be shown that the solutions of (2.5) are given by the expressions

$$X(x)=\begin{cases}\cos(k_{1x}x), & \text{for}\quad |x|<w/2\\ \left(n_c^2/n_a^2\right)\cos\left(k_{1x}w/2\right)\exp[-\gamma_{2x}(|x|)-w/2], & \text{for}\quad |x|>w/2\end{cases} \tag{2.8}$$

$$Y(y)=\begin{cases}C[\cos(k_{4y}t)+(\gamma_{3y}/k_{4y})\sin(k_{4y}t)]\exp[\gamma_{5y}(y+t)], & \text{for}\quad y\in(-\infty,-t)\\ C[\cos(k_{4y}y)-(\gamma_{3y}/k_{4y})\sin(k_{4y}y)], & \text{for}\quad y\in(-t,0)\\ C\exp(-\gamma_{3y}y), & \text{for}\quad y\in(0,\infty)\end{cases}. \tag{2.9}$$

with C a (normalization) constant that will be specified latter, and k_{1x}, γ_{2x}, γ_{3y}, k_{4y} and γ_{5y} constants describing the harmonic part (k) and respectively the damped/evanescent part (γ) of the solutions in the various sectors of the waveguide configuration, and are given by the expressions

$$\begin{aligned} &k_{1x}^2=k_0^2n_c^2-\beta_1^2 \qquad \gamma_{2x}^2=\beta_1^2-k_0^2n_a^2 \qquad \gamma_{3y}^2=\beta_2^2-k_0^2n_b^2\\ &k_{4y}^2=k_0^2n_c^2-\beta_2^2 \qquad \gamma_{5y}^2=\beta_2^2-k_0^2n_a^2. \end{aligned} \tag{2.10}$$

Besides the analytic expression of the solutions (2.8) and (2.9) of the system (2.5), the boundary conditions also yield two transcendental equations for the constants β_1 and β_2:

$$\begin{aligned} &\arctan\left(\frac{n_c^2\gamma_{2x}}{n_a^2k_{1x}}\right)-k_{1x}\frac{w}{2}+p\pi=0\\ &\arctan\left(\frac{\gamma_{3y}}{k_{4y}}\right)+\arctan\left(\frac{\gamma_{5y}}{k_{4y}}\right)+q\pi=0 \end{aligned} \tag{2.11}$$

whose (numerical) solutions for $(p,q)\in\boldsymbol{N}\times\boldsymbol{N}$ will determine the values $\beta_0(p,q)$ of the propagation constant in the z-direction corresponding to the modes $E_{pq}{}^{x}$ of the electromagnetic field.

Once the different propagation modes of the electromagnetic field have been determined from the solutions of (2.11), propagation modes of the strip-loaded waveguide configuration in figure 1 can be obtained in the perturbative framework [13] from the corresponding modes of the fundamental waveguide configuration in figure 2 (and analyzed above) by considering that the dielectric constant of the strip-loaded waveguide has the form

$$n_{\mathrm{SLW}}^2(x,y)=n_0^2(x,y)+\delta n_{\mathrm{SLW}}^2(x,y) \tag{2.12}$$

where $n_0^2(x,y)$ is given by (2.2) and $\delta n_{\mathrm{SLW}}^2(x,y)$ is a (small) perturbation having the expression

$$\delta n_{\mathrm{SLW}}^2(x,y)=\begin{cases}n_c^2-n_a^2, & \text{for } (x,y)\in[(-\infty,w/2)\cup(w/2,\infty)]\times[(-\infty,-t)\cup(0,\infty)]\\ 0, & \text{in rest.}\end{cases} \tag{2.13}$$

The perturbative approach described above has a very simple pictorial and physical interpretation. What the dielectric constant perturbation (2.13) does is essentially to 'remove' the shaded regions of the structure in figure 2, such that the resulting structure becomes a rectangular waveguide of the refractive index n_c, grown on a substrate of the refractive index n_b and covered by a 'cladding' of the refractive index n_a, i.e. exactly the configuration shown in figure 1. Of course, for such an approach to be valid, the refractive indices of the waveguide structures must obey the conditions:

$$n_a^2 \gg \left|n_c^2 - n_a^2\right|, \qquad n_b^2 \gg \left|n_c^2 - n_a^2\right|, \tag{2.14}$$

which, fortunately, are almost always satisfied in the cases of practical interest.

Under these circumstances, to the first order of perturbation, the propagation constant of the strip-loaded waveguide depicted in figure 1 is given by the expression

$$\beta_{\mathrm{SLW}}^2 = \beta_0^2 + \delta\beta_{\mathrm{SLW}}^2 \tag{2.15}$$

where β_0 is the propagation constant of the fundamental structure in figure 2, and $\delta\beta^2{}_{\mathrm{SLW}}$ is the first-order correction to the β_0 corresponding to the perturbation $\delta n_{\mathrm{SLW}}^2(x, y)$ of the dielectric constant in (2.13). The correction $\delta\beta^2{}_{\mathrm{SLW}}$ in (2.15) is given by the familiar general expression from perturbative calculus:

$$\delta\beta_{\mathrm{SLW}}^2 = \left(k_0^2/C\right) \iint_{R^2} \delta n_{\mathrm{SLW}}^2(x, y) |\Psi(x, y)|^2 \, \mathrm{d}x \, \mathrm{d}y \tag{2.16}$$

with $\Psi(x, y)$ the full solution of the fundamental waveguide as given by (2.8) and (2.9), and with C the normalization constant—which is the same constant appearing in the separate solution (2.9)—having the expression

$$C = \iint_{R^2} |\Psi(x, y)|^2 \, \mathrm{d}x \, \mathrm{d}y. \tag{2.17}$$

Using (2.8) and (2.9), both the first-order correction (2.16) and the normalization constant in (2.17) can be calculated exactly, and their analytic expressions are given for reference purposes in appendix A.

3. The perturbative treatment of strip-loaded trapezoidal waveguides

Following a methodology similar to that used in the construction of the strip-loaded rectangular waveguide structure in figure 1 from the fundamental waveguide structure in figure 2, the strip-loaded trapezoidal waveguide depicted in figure 3 can be obtained from the strip-loaded rectangular waveguide structure in a straightforward manner.

The 'wings' of the trapezoidal structure are added to the rectangular waveguide by considering an additional perturbation $\delta n_T^2(x, y)$ in the dielectric constant of the latter such that the refractive index of these 'wings' is changed from n_a to n_c. The perturbation $\delta n_T^2(x, y)$ that changes the refractive index of the domains (AED) and (BCF) in figure 3 from n_a to n_c has the expression

$$\delta n_{\mathrm{T}}^2(x, y) = \begin{cases} n_c^2 - n_a^2, & \text{for} \quad (x, y) \in \Delta(\mathrm{AED}) \cup \Delta(\mathrm{BCF}) \\ 0, & \text{in rest} \end{cases}. \tag{3.1}$$

Under these circumstances, to the first order of (overall) perturbation, the propagation constant β_{T} of the trapezoidal waveguide structure in figure 3 will be given by the expression

$$\beta_{\mathrm{T}}^2 = \beta_0^2 + \delta\beta_{\mathrm{SLW}}^2 + \delta\beta_{\mathrm{T}}^2 \tag{3.2}$$

where the first-order correction $\delta\beta_{\mathrm{T}}^2$ has the general form

$$\delta\beta_{\mathrm{T}}^2 = \left(k_0^2/C\right) \iint_{R^2} \delta n_{\mathrm{T}}^2(x, y) |\Psi(x, y)|^2 \, \mathrm{d}x \, \mathrm{d}y \tag{3.3}$$

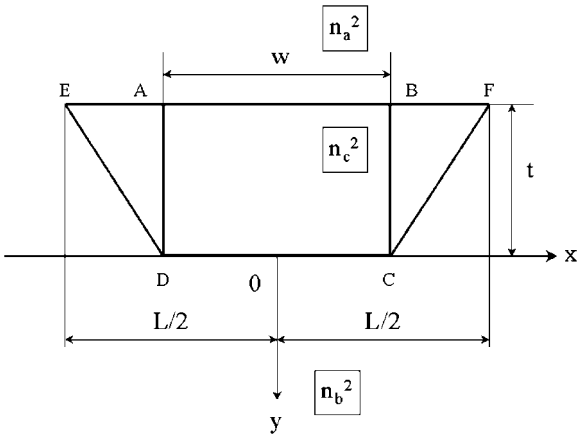

Figure 3. The cross-section of the trapezoidal waveguide obtained from the strip-loaded rectangular structure by adding the 'wings' (AED) and (BCF) with the refractive index n_c.

with all the symbols having the same significance as in (2.16). Analogous to the first-order correction in (2.16), the correction in (3.3) can also be calculated exactly, and its analytic expression is given for reference purposes in appendix B.

4. The perturbative propagation equivalence of the trapezoidal and rectangular strip-loaded waveguides

As was mentioned in section 1, it is possible to construct for any given trapezoidal waveguide, an equivalent rectangular waveguide that has to the first order of perturbation the same propagation constant as the original trapezoidal waveguide. The method underlying this construction was first developed in [3], and was briefly investigated numerically for the case of rib-waveguide structures[1]. In this section, we apply this method to the study of strip-loaded waveguide structures, and we show that in this latter case it yields a very simple geometrical criterion that allows one to construct the equivalent rectangular waveguide without recourse to any numerical calculations. The construction of the equivalent rectangular waveguide can be diagrammatically illustrated as in figure 4.

The fundamental idea behind the construction of an equivalent waveguide can be described as follows. Given the trapezoidal waveguide DEFC with the distribution of the refractive index as shown in figure 4, one constructs a rectangular waveguide GIMJ that has the same thickness t as the original trapezoidal waveguide and a width that has yet to be determined. The rectangular waveguide is constructed using the same method that was used in the previous sections, i.e. by appropriately perturbing the dielectric constant of the trapezoidal waveguide configuration, and the perturbation term corresponding to this construction has the general form

$$\delta n^2_{\mathrm{ER}}(x,y) = \begin{cases} n_c^2 - n_a^2 & \text{for} \quad (x,y) \in \Delta(\mathrm{HID}) \cup \Delta(\mathrm{CMK}) \\ -\left(n_c^2 - n_a^2\right) & \text{for} \quad (x,y) \in \Delta(\mathrm{HEG}) \cup \Delta(\mathrm{JFK}) \\ 0, & \text{in rest} \end{cases} . \tag{4.1}$$

[1] In the dedicated nomenclature, a rib-waveguide structure is a waveguide structure in which the waveguide and the substrate have the same refractive index/dielectric constant by contrast to the strip-loaded structures where the waveguide and the substrate have different refractive indices.

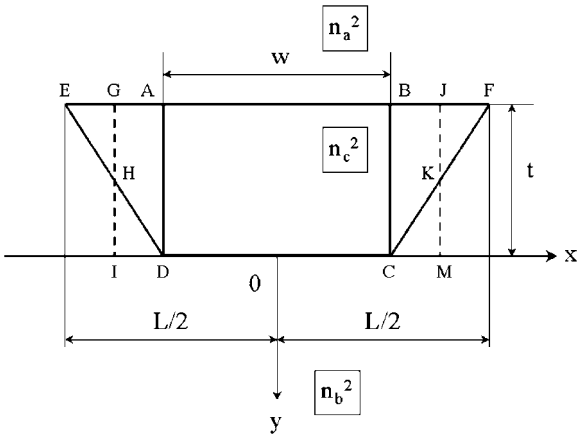

Figure 4. The construction of the equivalent rectangular waveguide GIMJ corresponding to the trapezoidal waveguide DEFC.

The perturbation (4.1) in the dielectric constant corresponds to a first-order correction $\delta\beta_{\mathrm{ER}}$ to the propagation constant of β_{T} of the trapezoidal waveguide having the general form

$$\delta\beta_{\mathrm{ER}}^2 = \left(k_0^2/C\right)\iint_{R^2}\delta n_{\mathrm{ER}}^2(x,y)|\Psi(x,y)|^2\,\mathrm{d}x\,\mathrm{d}y$$
$$= \frac{2k_0^2\left(n_c^2-n_a^2\right)}{C}\left\{\iint_{S_{\mathrm{HID}}}|\Psi(x,y)|^2\,\mathrm{d}x\,\mathrm{d}y - \iint_{S_{\mathrm{HEG}}}|\Psi(x,y)|^2\,\mathrm{d}x\,\mathrm{d}y\right\} \tag{4.2}$$

where the factor of 2 in the last equality on the rhs of (4.2) is once again due to the symmetry of the problem with respect to the y-axis, and with this correction the propagation constant of the rectangular waveguide GIMJ will be given to the first order by the expression

$$\beta_{\mathrm{ER}}^2 = \beta_0^2 + \delta\beta_{\mathrm{SLW}}^2 + \delta\beta_{\mathrm{T}}^2 + \delta\beta_{\mathrm{ER}}^2 = \beta_{\mathrm{T}}^2 + \delta\beta_{\mathrm{ER}}^2. \tag{4.3}$$

Due to the fact that the first-order correction $\delta\beta_{\mathrm{ER}}^2$ in (4.2) is given by the difference of two integrals, and since these two integrals will depend on the width of the rectangular waveguide GIMJ, it is possible to make this difference vanish by appropriately choosing the width of the waveguide. The vanishing of this difference implies the vanishing of the first-order correction $\delta\beta_{\mathrm{ER}}^2$, and consequently, it follows from (4.3) that to the first order the propagation constant β_{ER} of the rectangular waveguide GIMJ will be equal to the propagation constant β_{T} of the original trapezoidal waveguide DEFC.

This is the essence of the equivalent rectangular waveguide method; given a trapezoidal waveguide, one can construct an equivalent rectangular waveguide that has, to the first order, the same propagation constant as the original trapezoidal waveguide. The equivalent rectangular waveguide has the same thickness as the trapezoidal structure, and its width can be determined from the condition that the first-order correction (4.3) to the propagation constant vanishes. Indeed, by rewriting the latter condition in the more convenient form

$$\iint_{S_{\mathrm{HID}}}|\Psi(x,y)|^2\,\mathrm{d}x\,\mathrm{d}y - \iint_{S_{\mathrm{HEG}}}|\Psi(x,y)|^2\,\mathrm{d}x\,\mathrm{d}y = 0 \tag{4.4}$$

the two double integrals on the lhs of (4.4) can be calculated in a closed analytical form[2] and in doing so, one obtains a non-linear/transcendental equation whose unknown is the width of the equivalent rectangular waveguide and which can be solved numerically.

For the particular case of strip-loaded waveguide structures depicted in figure 4, one can avoid to solve equation (4.4) altogether by observing that $\Psi(x, y)$ has the same analytic expression on both integration domains S_{HID} and S_{HEG} in the two double integrals on the lhs of (4.4). Under these circumstances, (4.4) can be formally written as

$$\iint_{S_{\mathrm{HID}}-S_{\mathrm{HEG}}} |\Psi(x, y)|^2 \, \mathrm{d}x \, \mathrm{d}y = 0 \tag{4.5}$$

and it is not difficult to see that the integral in (4.5) will always vanish if the (areas of the) integration domains S_{HID} and S_{HEG} obey the condition

$$S_{\mathrm{HID}} = S_{\mathrm{HEG}}. \tag{4.6}$$

Furthermore, straightforward symmetry arguments allow one to re-express the condition (4.6) into a more geometrically meaningful form:

$$\Delta(\mathrm{HID}) \equiv \Delta(\mathrm{HEG}), \tag{4.7}$$

which requires the congruence of the two triangles bounding the integration domains S_{HID} and S_{HEG}, and this latter condition eliminates completely the need for numerically solving (4.4) by allowing one to determine the width of the equivalent rectangular waveguide from simple geometrical considerations. Indeed, it is not difficult to see from figure 4 that condition (4.7) implies that EG = GA, and under these circumstances, the width w' of the equivalent waveguide corresponding to a trapezoidal waveguide with the small base w and the large base L will be given by the expression

$$w' = \frac{w + L}{2}. \tag{4.8}$$

To summarize all the above considerations, given a trapezoidal waveguide of thickness t, small basis w and large basis L, with propagation modes determined perturbatively as described in the previous sections, it is possible to construct rectangular waveguide that has to the first-order of perturbation the same propagation constant (3.2)–(3.3) as the original trapezoidal waveguide. The equivalent rectangular waveguide has the same thickness as the trapezoidal waveguide, and its width (4.8) can be determined exactly from the simple geometrical condition (4.7) derived from the requirement that the two waveguides have the same propagation constant.

It should be noted that while the geometrical condition (4.7) and hence the expression (4.8) for the width of the equivalent rectangular waveguide were determined for the simpler case of an isosceles trapezoidal waveguide, the method described above can be easily generalized to the case of asymmetric trapezoidal waveguides. Indeed, in this latter case one only needs to apply separately condition (4.7) to each of the two (non-equal) wings of the trapezoidal profile, and the result will be an equivalent rectangular waveguide that is 'off-center', i.e. a rectangular waveguide whose vertical symmetry axis is displaced toward the 'wider' wing of the trapezoidal profile.

In view of the above propagation equivalence of the two waveguide structures, there is another way to determine the propagation constant of the equivalent rectangular waveguide

[2] Note that the authors of [3] appear to have chosen to solve (4.4) for their particular application by using a numerical method that involves the numerical integration of the two terms on the lhs of (4.4). Such a method is unnecessary in the opinion of the present authors, since for the geometries of interest—both in their case and ours—these integrals can be calculated analytically in a rather straightforward manner. Needless to say, the analytical calculation of these integral is always more desirable, since it eliminates any errors associated with numerical integration.

that avoids the direct calculation of the propagation constant of the trapezoidal structure, and as such it is much simpler.

Referring to figure 4, the equivalent rectangular waveguide GIMJ can be constructed directly from the rectangular waveguide ABCD by simply 'adding' perturbatively to the latter the lateral wings GADI and JBCM. The perturbation in the dielectric constant of the structure in figure 2 that is necessary for this operation is given by the expression

$$\delta n^2_{\mathrm{ERD}}(x,y) = \begin{cases} n_c^2 - n_a^2, & \text{for} \quad (x,y) \in S_{\mathrm{GADI}} \cup S_{\mathrm{JBCM}} \\ 0, & \text{in rest} \end{cases} \tag{4.9}$$

and the corresponding first-order correction to the propagation constant β_{SLW} in (2.15) and (2.16) will be given by the general expression

$$\begin{aligned} \delta\beta^2_{\mathrm{ERD}} &= \left(k_0^2/C\right) \iint_{R^2} \delta n^2_{\mathrm{ERD}}(x,y)|\Psi(x,y)|^2 \,\mathrm{d}x\,\mathrm{d}y \\ &= \frac{k_0^2\left(n_c^2 - n_a^2\right)}{C} \left\{ \iint_{S_{\mathrm{GADI}}} |\Psi(x,y)|^2 \,\mathrm{d}x\,\mathrm{d}y + \iint_{S_{\mathrm{JBCM}}} |\Psi(x,y)|^2 \,\mathrm{d}x\,\mathrm{d}y \right\} \\ &= \frac{2k_0^2\left(n_c^2 - n_a^2\right)}{C} \iint_{S_{\mathrm{GADI}}} |\Psi(x,y)|^2 \,\mathrm{d}x\,\mathrm{d}y \end{aligned} \tag{4.10}$$

where once more we have used the symmetry of the structures in figure 4 with respect to the y-axis in order to write the last equality in (4.10). It should be noted at this time that since the integration domains in (4.10) are rectangular, the analytical calculation of this correction is much simpler than the corresponding calculations for the correction term $\delta\beta^2_{\mathrm{T}}$. The explicit expression of the correction term in (4.10) is given for reference in appendix C, and with this correction term, the propagation constant of the equivalent rectangular waveguide will be given by the expression

$$\beta^2_{\mathrm{ERD}} = \beta_0^2 + \delta\beta^2_{\mathrm{SLW}} + \delta\beta^2_{\mathrm{ERD}} = \beta^2_{\mathrm{SLW}} + \delta\beta^2_{\mathrm{ERD}}. \tag{4.11}$$

The above expression for the propagation constant of the equivalent rectangular waveguide together with the corresponding expression in (4.3) will be used in the next section to test the numerical accuracy of this equivalence.

We conclude this section with a few considerations regarding the overall method we have used for the construction of the trapezoidal waveguide and for studying its propagation equivalence with the rectangular waveguide.

It should be mentioned that one could have used a different perturbative approach [3] to the construction of a trapezoidal waveguide from a 'fundamental' rectangular waveguide that involves the calculation of fewer correction terms. Such a method is illustrated in figure 5, and in a certain sense it represents the inverse of the method we have used so far.

The strip-loaded waveguide ABCD is obtained as before from a 'fundamental' rectangular waveguide of the type depicted in figure 2, and is considered to be already the 'equivalent' waveguide. The trapezoidal structure EGHF (whose geometrical dimensions are supposed to be known) is then constructed from the waveguide ABCD as indicated in figure 2, and the entire construction needs to satisfy the condition that the width of the rectangular structure should be smaller than the small basis GH of the trapezoidal profile. It should be noted that in this approach the width of the rectangular waveguide is unknown, and as such it will appear as a parameter in all the calculations (e.g. general form of the solutions, boundary conditions and more importantly, modal equations) required for the construction of this structure from a 'fundamental' structure of the type illustrated in figure 2.

The explicit value of this width will be determined from the requirement that the two waveguide structures have the same propagation constant to the first order of perturbation, and

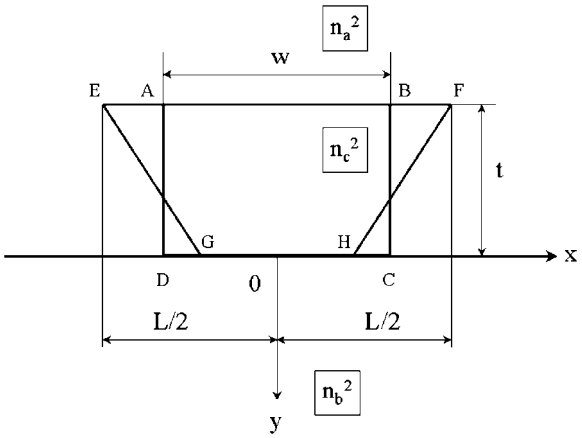

Figure 5. Alternative construction of a trapezoidal waveguide from the strip-loaded waveguide configuration in figure 1.

this requirement will result in an equation similar to (4.4). However, due to the above considerations, this equation will be extremely complicated and will necessarily require numerical methods for its solutions. Furthermore, since the width also determines the 'vertical' modes of the waveguide, and since the corresponding modal equation in (2.11) also requires numerical solutions, one has, in fact, to solve numerically not a single equation but a system of transcendental equations.

For these reasons, and as explained in section 1, we have chosen not to use such an approach, but instead we have decided to use the approach described in the present and earlier sections, which has the major advantage that it offers a simple and exact method for the determination of the width of the equivalent rectangular waveguide that does not require any numerical calculations.

5. Numerical results and discussion

For the numerical investigation of the theoretical consideration presented in the previous settings, we have chosen two trapezoidal waveguide structures, which for notational simplicity have been labeled as T_1 and T_2. Both these trapezoidal structures are geometrically similar, in the sense that they are structures with the same w, same angle for the sides (32°) but different heights. The explicit geometrical and physical properties of these two structures are as follows. For T_1 we have chosen $w = 2$ μm, $t = 0.73$ μm, $L = 4.34$ μm, for T_2 we have chosen $w = 2$ μm, $t = 1.07$ μm, $L = 5.42$ μm, and both waveguide configurations have refractive index distributions that are specific to InP/InGaAsP SOA structures [9], i.e. $n_a = 1$, $n_b = 1.538$, $n_c = 1.568$. The dimensions and physical properties of the equivalent rectangular structures corresponding to T_1 and respectively T_2 can easily be determined by using the arguments presented in the previous sections. All the results that will be presented in the following are based on the analytical considerations presented in the previous sections and in the corresponding appendices, and all the numerical calculations involved in obtaining these results have been performed using *MathCad 2000 Professional*.

As a first test of the validity and accuracy of the propagation equivalence between trapezoidal waveguides and their rectangular counterparts we have considered the dispersion

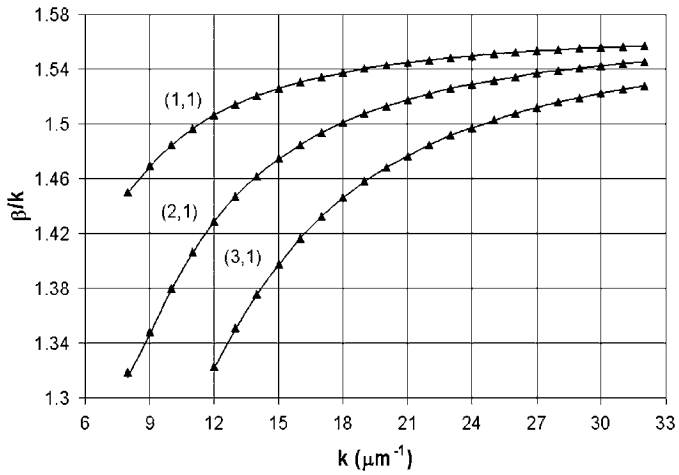

Figure 6. Dispersion curves for the trapezoidal structure T_1 (continuous line) and its equivalent rectangular structure (trapezoidal marker). The modes (p, q) are indicated above each pair of curves.

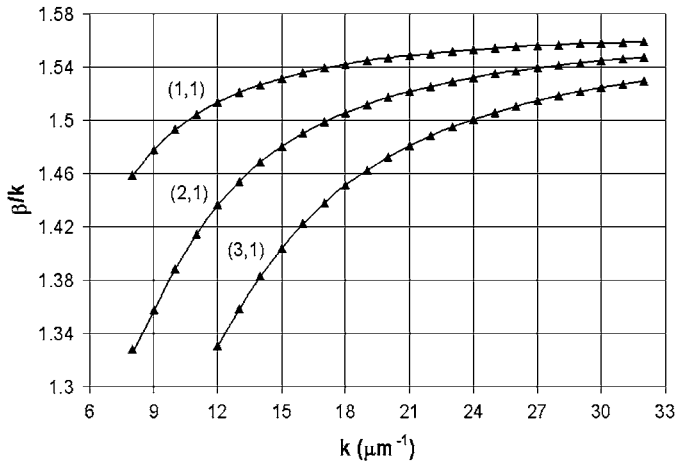

Figure 7. Dispersion curves for the trapezoidal structure T_2 (continuous line) and its equivalent rectangular structure (trapezoidal marker). The modes (p, q) are indicated above each pair of curves.

data β/k versus k for various propagation modes (p, q) of these structures. Since from the theoretical standpoint the dominant mode for trapezoidal waveguides is the (1, 1) mode [1], and since from the experimental viewpoint it appears that the (1, 1) mode is the lowest mode supported by such structures [5], we have restricted our numerical analysis only to propagation modes with $p, q \geqslant 1$. Explicitly, we have chosen for our investigation the modes with $p = 1$, 2, 3 and $q = 1$, and we have compared the dispersion curves β_T/k versus k of the structures T_1 and T_2 with the dispersion curves β_{ERD}/k versus k of the corresponding equivalent rectangular structures.

The results are presented in figures 6 and 7, and as it can be seen from these figures, for both structures T_1 and T_2 the dispersion curves for the modes under consideration are in

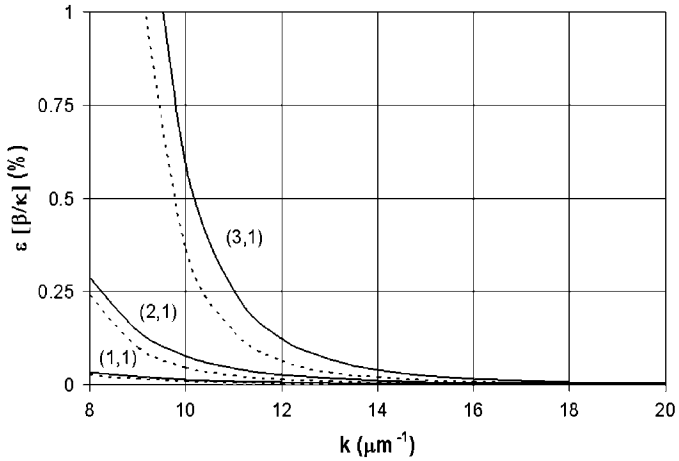

Figure 8. Relative error with which the equivalent rectangular waveguides reproduce the dispersion curves of the trapezoidal structures T_1 (continuous line) and T_2 (dotted line). The modes (p, q) are indicated above each pair of curves.

excellent agreement with the corresponding dispersion curves of their respective equivalent rectangular counterparts.

For each mode, the dispersion curves practically overlap, and the overlapping precision/relative error per point is illustrated in figure 8.

From the analysis of figure 8 one can draw the following conclusions. First of all, the accuracy with which the equivalent rectangular waveguides reproduce the dispersion curves of the trapezoidal waveguides is the highest for the dominant mode (1, 1) and decreases for higher modes. In particular, for the modes under consideration, the maximum overlapping error increases by about one order of magnitude with increasing order p of the mode, reaching the value of 2.4465% (not shown in the graph) for the mode (3, 1) of the structure T_1.

Second, the overlapping error for each mode is larger for the structure T_1 than for the structure T_2, suggesting that since the two structures are geometrically similar as mentioned earlier, the overlapping error decreases with increasing thickness t of the waveguide structure.

Finally, the overlapping error for each mode decreases significantly with increasing wavenumber k, in the sense that for each of the structures T_1 and T_2 the overlapping error at high values of $\underline{k}$ becomes at least two orders of magnitude smaller than the maximum error of the respective mode.

As a second test of the validity and accuracy of the propagation equivalence between trapezoidal waveguides and their rectangular counterparts we have considered the data describing the variation of the effective refractive index β/k for the various propagation modes (p, q) of these structures with respect to the size L of the large basis of the trapezoidal structures. Explicitly, we use the same propagation modes as before, and for each mode we compare the curves β_T/k versus L of the structures T_1 and T_2 with the curves β_{ERD}/k versus L of the corresponding equivalent rectangular structures. In all of the following, for notational simplicity, we will continue to use the notation T_1 and T_2 to designate the two (sets of) trapezoidal structures under consideration, with the implicit understanding that with the exception of the value of the large basis L of these structures, all the other geometrical

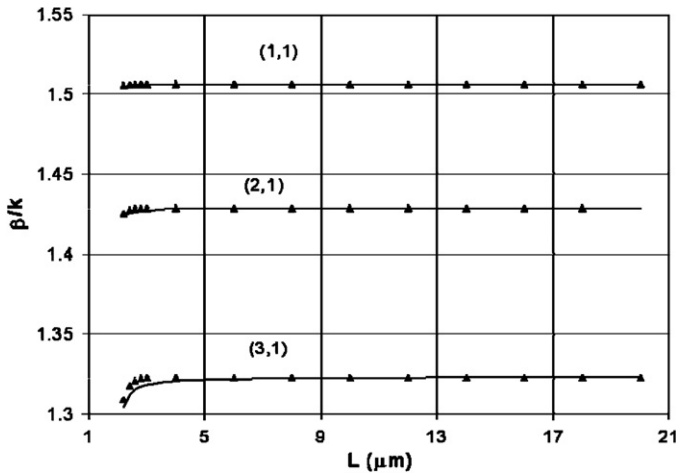

Figure 9. Plot of the curves β_T/k versus L for the structures T_1 and the curves β_{ERD}/k versus L for the corresponding equivalent rectangular structures. The modes (p, q) are indicated above each pair of curves.

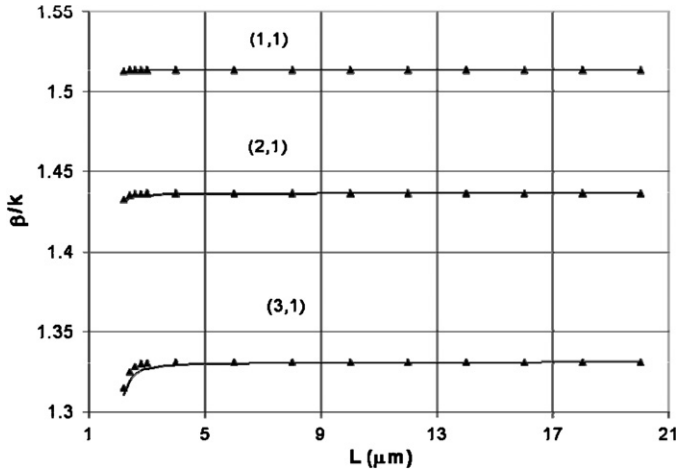

Figure 10. Plot of the curves β_T/k versus L for the structures T_2 and the curves β_{ERD}/k versus L for the corresponding equivalent rectangular structures. The modes (p, q) are indicated above each pair of curves.

and physical properties of these structures remain unchanged and have the values mentioned earlier.[3]

The results are presented in figures 9 and 10 and very much like in the case of the dispersion curves, the curves of the equivalent rectangular structures are in excellent agreement with the corresponding curves of the trapezoidal structures T_1 and T_2 respectively.

[3] Under these circumstances, the difference between the two set of structures T_1 and T_2 (and of course the difference between the corresponding equivalent waveguides) lies—apart from the variation of the size L of the large basis of the structures—in the different thicknesses t of these structures. According to the considerations in the beginning of the present section, the structures T_1 are characterized by a thickness $t = 0.73$ μm, while the structures T_2 are characterized by a thickness $t = 1.07$ μm.

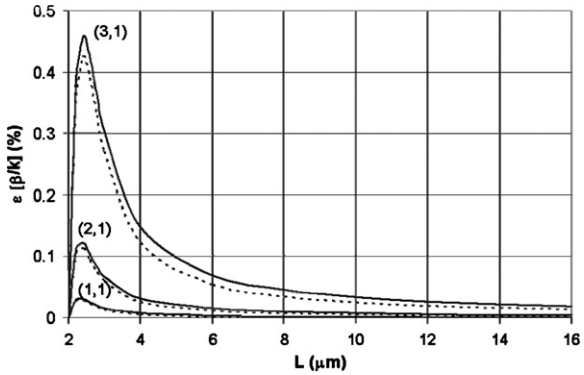

Figure 11. Relative error with which the equivalent rectangular waveguides curves β_{ERD}/k versus L reproduce the curves β_{T}/k versus L of the trapezoidal structures T_1 (continuous line) and T_2 (dotted line). The modes (p, q) are indicated above each pair of curves.

For each of the modes under consideration, the overlapping precision/relative error per data point is illustrated in figure 11.

The conclusions drawn from the analysis of figure 11 are similar in trend to those obtained from the analysis of figure 8. Indeed, as it can be seen from figure 11, the accuracy with which the equivalent rectangular waveguides reproduce the dispersion curves of the trapezoidal waveguides is the highest for the dominant mode (1, 1) and decreases for higher modes, the overlapping error for each mode is larger for the structures T_1 than for the structures T_2 suggesting that the error increases with increasing thickness t of the waveguide structure, the maximum overlapping error increases with increasing order p of the mode and the overlapping error for each mode decreases with increasing wavenumber k.

However, it should be noted that while the graphs in figures 11 and 8 show similar qualitative trends, quantitatively they are different in at least one significant aspect. The most important difference rests with the maximum error for the higher modes, and it is clear that for both sets of structures T_1 and T_2 the maximum error is smaller in figure 11 than in figure 8.

The reduction in the maximum error for these modes is by a factor of approximately 2 for the (2, 1) mode and approximately 6 for the mode (3, 1). Interestingly enough, for the dominant mode (1, 1) the maximum error has essentially the same value in both graphs. Under these circumstances, we can safely say that the equivalent rectangular structures reproduce the curves β_{T}/k versus L of the corresponding trapezoidal structures more accurately than they reproduce the dispersion curves β_{T}/k versus k.

It should also be noted that the curves in figure 11 show a particularly interesting and important feature, namely the fact that for each mode, as the size of the large basis L decreases, the overlapping error reaches a maximum value followed by a rapid drop to zero as L approaches the value of the small basis w of the trapezoidal structures.

The rapid drop to zero of the overlapping error as L approaches w has a very intuitive and natural geometrical explanation, representing in fact a proof of validity for our method. Indeed, referring to figure 4, as the size L of the large basis of the trapezoidal structures approaches the value of the small basis w of these structures, one would expect that both the trapezoidal structures DEFC and the corresponding equivalent rectangular structures GIMJ would approach the geometry and size of the structure ABCD. When $L = w$, all these three structures should become identical, under which circumstances they should all be characterized

by the propagation constant β_{SLW} of the waveguide ABCD. As it can be seen from figure 11, this intuitive line of reasoning is fully supported by the numerical results, and needless to say, it is also fully supported by the analytic results presented in the previous sections and in the appendices. Indeed, it is not difficult to verify that for $L \to w$ both first-order corrections $\delta\beta_T$ and $\delta\beta_{ERD}$ approach zero, such that in the limit $L = w$ we obtain $\beta_T = \beta_{ERD} = \beta_{SLW}$, i.e. we recover the intuitive geometrical result described above that in this limit both structures DEFC and GIMJ become identical to—and will have the same value β_{SLW} for the propagation constant as—the structure ABCD.

However, the above-mentioned feature that is important for the purpose of our present work—and surprising at the same time—is not the rapid drop to zero of the overlapping error as $L \to w$, but rather the existence of a global maximum of this error for each mode. The existence of such a global maximum is extremely important indeed, because it offers for each propagation mode an overall lower bound for the accuracy with which the present method can be applied to the description of the propagation characteristics of trapezoidal waveguides.

Summarizing the considerations and results in this section, the error with which the perturbative propagation equivalence method developed in the present paper reproduces the propagation characteristics of trapezoidal waveguides depending on the geometrical properties of these waveguides, the wavevector k of the radiation propagating through it and the propagation mode under consideration. Typical values for this error range from below 0.05% for the dominant mode of the waveguide to approximately 3% for the highest mode that has been investigated, and based on these results we can conclude with confidence that this method offers a highly accurate alternative for the description of the propagation characteristics of lossless trapezoidal waveguides.

6. Conclusions

In the present paper we have considered the method of first-order propagation equivalence between trapezoidal and rectangular strip-loaded waveguides, and we have developed a new and improved version of this method. The version we have developed has the advantage of being much simpler both at the conceptual level and at the mathematical level. At the conceptual level it offers an extremely simple geometrical method for the (perturbative) construction of a propagationally equivalent rectangular structure for any given trapezoidal waveguide, while at the same time it allows for a mathematical description that is mostly analytical and requires only minimal use of numerical analysis methods. The numerical investigation carried out to test the accuracy of our method shows it to be in excellent agreement with the perturbative description of trapezoidal waveguides, confirming the validity of our approach.

It should be noted that while the work carried out in this paper has been restricted only to the description of lossless trapezoidal waveguides, it can be straightforwardly generalized to include the effects of material loss by considering complex propagation constants β and by carrying out the calculations in the complex plane. Under these circumstances, the method can be applied to the study of the properties of SOAs with trapezoidal cross-sections, which is an issue that will be addressed in a future paper.

It is also very important to emphasize that mathematical description aside, the present work has important and immediate applications in the numerical modeling of optoelectronic devices. In particular, it is especially useful for extending the applicability range of already existing commercial simulation software—which generally relies on models of rectangular cross-section devices—to include structures whose cross-section is trapezoidal, allowing for more accurate designs of complex optoelectronic systems.

Appendix A. The normalization constant and the first-order correction $\delta\beta^2_{\mathrm{SLW}}$ for the strip-loaded rectangular waveguide

As mentioned in section 2, the normalization constant C required for the quantitative evaluation of the first-order correction to the propagation constant β_0 is given by the general expression

$$C = \iint_{R^2} |\Psi(x, y)|^2 \, \mathrm{d}x \, \mathrm{d}y \tag{A.1}$$

where the integral is over the entire two-dimensional surface containing the waveguide cross-section, and $\Psi(x, y)$ is the full solution of the scalar-wave equation (2.1) as determined by (2.8) and (2.9).

The calculation of the normalization constant is quite straightforward, and requires the splitting of the double integral in (A.1) into several integrals corresponding to the expressions of the solution $\Psi(x, y)$ on the various spatial domains of relevance. Under these circumstances, it can be shown that in fact we can write

$$C = \sum_{i=1}^{9} J_i \tag{A.2}$$

where the terms/integrals J_i on the rhs of (A.2) have the expressions

$$J_1 = \int_{-\infty}^{-w/2} \mathrm{d}x \int_{-\infty}^{-t} \mathrm{d}y |\Psi(x, y)|^2 = \frac{D_{12}^2}{4\gamma_{2x}\gamma_{5y}} \tag{A.3}$$

$$J_2 = \int_{-\infty}^{-w/2} \mathrm{d}x \int_{-t}^{0} \mathrm{d}y |\Psi(x, y)|^2 = \left(\frac{D_1^2}{4\gamma_{2x}}\right) \left\{ t \left[1 + \left(\frac{\gamma_{3y}}{k_{4y}}\right)^2 \right] + \left(\frac{\gamma_{3y}}{k_{4y}^2}\right) [1 - \cos(2k_{4y}t)] \left(\frac{1}{k_{4y}}\right) \left[1 - \left(\frac{\gamma_{3y}}{k_{4y}}\right)^2 \right] \sin(2k_{4y}t) \right\} \tag{A.4}$$

$$J_3 = \int_{-\infty}^{-w/2} \mathrm{d}x \int_{0}^{\infty} \mathrm{d}y |\Psi(x, y)|^2 = \frac{D_1^2}{4\gamma_{2x}\gamma_{3y}} \tag{A.5}$$

$$J_4 = \int_{-w/2}^{w/2} \mathrm{d}x \int_{-\infty}^{-t} \mathrm{d}y |\Psi(x, y)|^2 = \frac{D_2^2}{4\gamma_{5y}} \left[w + \frac{\sin(k_{1x}w)}{k_{1x}} \right] \tag{A.6}$$

$$J_5 = \int_{-w/2}^{w/2} \mathrm{d}x \int_{-t}^{0} \mathrm{d}y |\Psi(x, y)|^2 = \left(\frac{J_2 J_4}{4}\right) \left(\frac{16\gamma_{2x}\gamma_{5y}^2}{D_{12}^2 D_2^2}\right) \tag{A.7}$$

$$J_6 = \int_{-w/2}^{w/2} \mathrm{d}x \int_{0}^{\infty} \mathrm{d}y |\Psi(x, y)|^2 = \frac{1}{4\gamma_{3y}} \left[w + \frac{\sin(k_{1x}w)}{k_{1x}} \right] \tag{A.8}$$

$$J_7 = \int_{w/2}^{\infty} \mathrm{d}x \int_{-\infty}^{-t} \mathrm{d}y |\Psi(x, y)|^2 = J_1 \tag{A.9}$$

$$J_8 = \int_{\mathrm{w}/2}^{\infty} \mathrm{d}x \int_{-\mathrm{t}}^{0} \mathrm{d}y |\Psi(x, y)|^2 = J_2 \tag{A.10}$$

$$J_7 = \int_{w/2}^{\infty} \mathrm{d}x \int_{0}^{\infty} \mathrm{d}y |\Psi(x, y)|^2 = J_3 \tag{A.11}$$

where in (A.3)–(A.11) we have used the notations

$$D_1 = \left(\frac{n_c}{n_a}\right)^2 \cos\left(\frac{k_{1x}w}{2}\right) \tag{A.12}$$

$$D_2 = \cos(k_{4y}t) + \left(\frac{\gamma_{3y}}{k_{4y}}\right)\sin(k_{4y}t) \tag{A.13}$$

$$D_{12} = D_1 D_2. \tag{A.14}$$

It should be noted at this time that the results for J_7 –J_9 in (A.9)–(A.11) reflect the symmetry of the solutions of the scalar-wave equation with respect to the x-axis, and under these circumstances (A.2) can be rewritten in the simpler form

$$C = 2\,(J_1 + J_2 + J_3) + J_4 + J_5 + J_6. \tag{A.15}$$

With these considerations, one can immediately calculate the first-order correction to the propagation constant β_0. According to (2.16), the general form for this correction term is given by the expression

$$\delta\beta^2_{\mathrm{SLW}} = \left(k_0^2/C\right)\iint_{R^2} \delta n^2_{\mathrm{SLW}}(x, y)|\Psi(x, y)|^2\,\mathrm{d}x\,\mathrm{d}y \tag{A.16}$$

and by using the explicit form (2.13) of the perturbation in the dielectric constant, it can be shown that (A.16) can be written in the form

$$\delta\beta^2_{\mathrm{SLW}} = \frac{2k_0^2\left(n_c^2 - n_a^2\right)}{C}\,[J_1 + J_3] = \frac{k_0^2\left(n_c^2 - n_a^2\right)}{2C\gamma_{2x}}\left[\frac{D_{12}^2}{\gamma_{5y}} + \frac{D_1^2}{\gamma_{3y}}\right]. \tag{A.17}$$

Appendix B. The first-order correction to $\delta\beta^2_{\mathrm{T}}$ for the strip-loaded trapezoidal waveguide

The first-order correction $\delta\beta^2_{\mathrm{T}}$ has the general form

$$\delta\beta^2_{\mathrm{T}} = \left(k_0^2/C\right)\iint_{R^2} \delta n^2_{\mathrm{T}}(x, y)|\Psi(x, y)|^2\,\mathrm{d}x\,\mathrm{d}y \tag{B.1}$$

where the perturbation in the dielectric constant $\delta n^2_{\mathrm{T}}(x, y)$ is given by (3.1), and the full solution $\Psi(x, y)$ of the scalar-wave equation is obtained from (2.8) and (2.9). Using now the explicit from of $\delta n^2_{\mathrm{T}}(x, y)$, (B.1) can be rewritten in the form

$$\delta\beta^2_{\mathrm{T}} = \frac{k_0^2\left(n_c^2 - n_a^2\right)}{C}\left\{\iint_{S_{\mathrm{AED}}} |\Psi(x, y)|^2\,\mathrm{d}x\,\mathrm{d}y + \iint_{S_{\mathrm{BCF}}} |\Psi(x, y)|^2\,\mathrm{d}x\,\mathrm{d}y\right\} \tag{B.2}$$

where S_{AED} and S_{BCF} are the areas of the surfaces bound by the triangles Δ(AED) and respectively Δ(BCF). Using the symmetry properties of the full solutions $\Psi(x, y)$ with respect to the y-axis, it follows immediately that if $\Delta(\mathrm{AED}) \equiv \Delta(\mathrm{BCF})$—i.e. if the trapezoidal cross-section in figure 3 is also symmetric with respect to the y-axis—then the rhs of (B.2) can be further simplified such that the expression of the first-order correction $\delta\beta^2_{\mathrm{T}}$ becomes

$$\delta\beta^2_{\mathrm{T}} = \frac{2k_0^2\left(n_c^2 - n_a^2\right)}{C}\iint_{S_{\mathrm{AED}}} |\Psi(x, y)|^2\,\mathrm{d}x\,\mathrm{d}y. \tag{B.3}$$

In order to be able to calculate analytically the surface integral on the rhs of (B.3), it is necessary to rewrite it with the appropriate integration limits corresponding to the geometry of the surface S_{AED}. This is not very difficult to do, and it can be shown that in fact the integration limits in the surface integral are explicitly

$$\iint_{S_{\mathrm{AED}}} |\Psi(x, y)|^2\,\mathrm{d}x\,\mathrm{d}y = \int_{-L/2}^{-w/2}\mathrm{d}x\int_{-t}^{ax+b}\mathrm{d}y|\Psi(x, y)|^2 \tag{B.4}$$

where $y = ax + b$ is the equation of the side DE of the triangle Δ(ADE). Using simple analytical geometry, it can be shown that the coefficients a and b that appear in the equation of the line DE have the expressions

$$a = \frac{2t}{L-w}, \qquad b = \frac{wt}{L-w}. \tag{B.5}$$

With (B.5), and after a few mathematical manipulations, the expression for the correction $\delta\beta_{\mathrm{T}}^2$ can be put in the final form for the present purposes:

$$\delta\beta_{\mathrm{T}}^2 = \frac{2k_0^2 D_1^2 \left(n_c^2 - n_a^2\right)}{C} \sum_{j=1}^{4} K_j \tag{B.6}$$

where the terms K_j of the sum on the rhs of (B.6) have the expressions

$$K_1 = \left(\frac{a}{8\gamma_{2x}}\right)\left[1 + \left(\frac{\gamma_{3y}}{k_{4y}}\right)^2\right]\left\{L\exp\left[\gamma_{2x}\,(w-L)\right] - w - \left(\frac{1}{\gamma_{2x}}\right)\{1 - \exp[\gamma_{2x}(w-L)]\}\right\} \tag{B.7}$$

$$K_2 = \left(\frac{1}{4\gamma_{2x}}\right)\left\{(b+t)\left[1 + \left(\frac{\gamma_{3y}}{k_{4y}}\right)^2\right] - \left(\frac{\gamma_{3y}}{k_{4y}^2}\right)\cos(2k_{4y}t) + \left(\frac{1}{2k_{4y}}\right)\left[1 - \left(\frac{\gamma_{3y}}{k_{4y}}\right)^2\right]\sin(2k_{4y}t)\right\}\{1 - \exp\left[\gamma_{2x}\,(w-L)\right]\} \tag{B.8}$$

$$K_3 = \left[\frac{\gamma_{3y}}{4k_{4y}^2\left(a^2k_{4y}^2 + \gamma_{2x}^2\right)}\right]\{\gamma_{2x}\cos(2ak_{4y}w - 2k_{4y}b) - ak_{4y}\sin(2ak_{4y}w - 2k_{4y}b) - [\gamma_{2x}\cos(2ak_{4y}L - 2k_{4y}b) - ak_{4y}\sin(2ak_{4y}L - 2k_{4y}b)]\exp[\gamma_{2x}(w-L)]\} \tag{B.9}$$

$$K_3 = \left[\frac{1 - \left(\frac{\gamma_{3y}}{k_{4y}}\right)^2}{4k_{4y}\left(a^2k_{4y}^2 + \gamma_{2x}^2\right)}\right]\{-[\gamma_{2x}\sin(2ak_{4y}w - 2k_{4y}b) + ak_{4y}\cos(2ak_{4y}w - 2k_{4y}b)] + [\gamma_{2x}\sin(2ak_{4y}L - 2k_{4y}b) + ak_{4y}\cos(2ak_{4y}L - 2k_{4y}b)]\exp[\gamma_{2x}(w-L)]\}. \tag{B.10}$$

Appendix C. The direct calculation of the propagation constant β_{ERD} for the equivalent rectangular waveguide

As mentioned in section 4, the propagation constant of the equivalent rectangular waveguide GIMJ in figure 4 can be calculated directly by using the relation

$$\beta_{\mathrm{ERD}}^2 = \beta_0^2 + \delta\beta_{\mathrm{SLW}}^2 + \delta\beta_{\mathrm{ERD}}^2 = \beta_{\mathrm{SLW}}^2 + \delta\beta_{\mathrm{ERD}}^2 \tag{C.1}$$

where β_{SLW}^2 is given by (2.15)–(2.17) and the correction term $\delta\beta_{\mathrm{ERD}}^2$ is given by the expression in (4.10):

$$\delta\beta_{\mathrm{ERD}}^2 = \frac{2k_0^2\left(n_c^2 - n_a^2\right)}{C}\iint_{S_{\mathrm{GADI}}} |\Psi(x,\,y)|^2\,\mathrm{d}x\,\mathrm{d}y. \tag{C.2}$$

The integral on the rhs of (C.2) can be calculated straightforwardly in a closed analytical form, and it can be shown that eventually the first-order correction $\delta\beta_{\mathrm{ERD}}^2$ is given by the

expression

$$\delta\beta^2_{\mathrm{ERD}} = \frac{2k_0^2\left(n_c^2 - n_a^2\right)}{C}\int_{-(L+w)/4}^{-w/2} \mathrm{d}x \int_{-t}^{0} \mathrm{d}y |\Psi(x, y)|^2 \,\mathrm{d}x\,\mathrm{d}y$$
$$= \frac{k_0^2\left(n_c^2 - n_a^2\right)D_1^2}{C\gamma_{2x}}\left\{\frac{t}{2}\left[1 + \left(\frac{\gamma_{3y}}{k_{4y}}\right)^2\right] + \frac{1}{4k_{4y}}\left[1 - \left(\frac{\gamma_{3y}}{k_{4y}}\right)^2\right]\sin(2k_{4y}t)\right.$$
$$\left. + \frac{\gamma_{3y}}{2k_{4y}^2}[1 - \cos(2k_{4y}t)]\right\}\left\{1 - \exp\left[\frac{\gamma_{2x}}{2}(w - L)\right]\right\} \tag{C.3}$$

where the normalization constant C and D_1 are given in explicit form in appendix A.

References

[1] Xu F, Zhao K, You B and Lin X 2000 *Int. J. Infrared Millim Waves* **21** 45
[2] Kitamura S, Komatsu K and Kitamura M 1998 *IEEE Photonics Technol. Lett* **6** 173
[3] Clark D F and Dunlop I 1967 *Electron. Lett* **24** 1414
[4] Muilwyk C A and Davies J B 1967 *IEEE Trans. Microw. Theory Tech.* **15** 450
[5] Pelosi P M, Vandenbulcke P, Wilkinson C D W and De La Rue R M 1978 *Appl. Opt.* **17** 1187
[6] Miyamoto T 1980 *Opt. Commun.* **34** 35
[7] Gillner L 1992 *IEE Proc.-J.* **139** 339
[8] Marcuse D 1983 *IEEE J. Quantum Electron.* **19** 63
[9] Connelly M J 2001 *IEEE J. Quantum Electron.* **37** 439
[10] Kumar A, Thyagarajan K and Ghatak A K 1983 *Opt. Lett.* **8** 63
[11] Varshney R K and Kumar A 1988 *J. Lightwave Technol.* **6** 601
[12] Marcuse D 1981 *Theory of Dielectric Optical Waveguides* 2nd edn (Edinburgh: Academic)
[13] Adams M J 1981 *An Introduction to Optical Waveguides* (New York: Wiley)
[14] Marcatili E A J and Miller S E 1969 *Bell Syst. Tech. J.* **48** 2161